Journal of
Bioengineering & Biomedical Science
ISSN: 2155-9538

Research Article

Open Access

Transitioning from Saccade to Smooth Pursuit Eye Movements using Linear Quadratic Tracking Control

Korentis GA and Enderle JD*

Department of Biomedical Engineering, University of Connecticut, Storrs, Connecticut 06269-3247, USA

Abstract

An optimal linear quadratic tracking controller (LQTC) which emulates smooth pursuit eye movements has been shown to accurately track various motion profiles in the presence of neural transmission delays. However, the initial orientation of the eye relative to the location of where a target first becomes salient affects the time course in which the desired trajectory is fully acquired. It is shown that a control strategy that incorporates a latent saccade to rapidly reposition the gaze to a predicted point on the trajectory path, then transitions the engagement smoothly using the LQTC, produces eye movements consistent with experimental observations.

Keywords: Eye movements; Smooth pursuit; Saccades; Optimal control; Motor control delay; Linear quadratic tracking; Lyapunov stability

Introduction

Using the principles of optimality, it was shown that a linear quadratic tracking controller (LQTC) could overcome the destabilizing effects of neural transmission delays to track a reference trajectory for a simple second order model of the oculomotor plant [1]. The caveat was that the initial position of the eye needed to be close to the starting location of the trajectory in order to achieve minimal tracking error in a timely fashion. Eye orientations starting away from the onset of the movement produced reliable tracking, but at synchronization times well outside the experimentally observed data for smooth pursuit eye movements as shown in Figure 1 for two different motion profiles.

This observation came as no surprise since the LQTC was designed to specifically emulate smooth pursuit eye movements which are relatively slow and have a maximum velocity range of 70°/s to 100°/s [2-5]. This was accomplished using the principles of optimality in which the minimization of performance criteria establishes a tradeoff between the weighted sum of control effort and the weighted sum of the error associated with the desired and measured state trajectories, which are constrained by the oculomotor dynamics. Since the design intent of the controller was to accurately track a moving target in the wake of large position state feedback delays, the time response of the LQTC can only perform so fast before driving the system towards instability. In other words, the controller was not designed for the ballistic repositioning of gaze but for smooth trajectory following within the physiological limitations of the oculomotor system.

Saccades

A smooth pursuit eye movement is preceded by what is commonly referred to as a catch-up saccade [2,6]. This is a fast eye movement that functions to rapidly reposition the eye from its current location to a predicted target location without concern for image formation on the retina [4,5,7]. As a matter of survival, evolution has equipped us with a ballistic targeting system that allows us to observe our environment more intently. There is sufficient evidence supporting the notion that saccades operate under open loop, time-optimal control [4,8-15]. Intuitively, this makes sense since the goal of a saccade is to foveate[1] a target as fast as possible.

Important parameters associated with a saccade are its magnitude, latency, peak velocity and duration. Figure 2 represents the typical characteristics of a 10° express saccade that has a latency of 100 ms. This is the time required for the oculomotor system to compute the error between the eye's current position and the target position [16-18]. It then generates the neural commands necessary to make the movement.

Visually guided, horizontal saccades are generally evaluated using the Main Sequence Diagrams [4,19]. These diagrams show the general relationship between a saccade's magnitude and its peak velocity, duration and latent period as shown in Figure 3 (Adopted from) [4].

Using the Main Sequence Diagrams, we created a control strategy that incorporates the timing of a physiologically realistic saccade to rapidly position the eye to a predicted target location on the trajectory, then engage and track the motion profile using the LQTC.

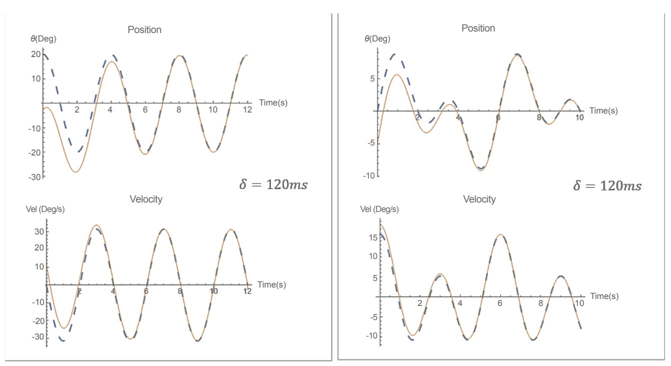

A) $\theta_d = 20°Cos\left(\frac{\pi}{2}t\right)$; $\theta_o = -3°$ B) $\theta_d = Sin\left(\frac{2\pi}{6}t\right) + Sin\left(\frac{2\pi}{3}t\right)$; $\theta_o = -5°$

Figure 1: Effects of initial eye position on the time course of target acquisition for the LQTC with a 150 ms position state feedback delay.

[1]The retina is made of up two very different types of photoreceptor cells. Rod cells are light and motion sensitive but have very low spatial resolution and make up the majority of the retina. Cone cells, on the other hand, are color sensitive, have very high spatial acuity and are densely packed in a very small region of the retina ($\cong \phi$ 1.2 mm) called the fovea. The process of moving the eye such that image formation may occur on this region is called foveation.

***Corresponding author:** Enderle JD, Department of Biomedical Engineering, University of Connecticut, 260 Glenbrook Road, Storrs, Connecticut 06269-3247, USA, Tel: 1860-486-5521; E-mail: jenderle@engr.uconn.edu

Received: May 13, 2016; **Accepted:** May 25, 2016; **Published**: June 06, 2016

Citation: Korentis GA, Enderle JD (2016) Transitioning from Saccade to Smooth Pursuit Eye Movements using Linear Quadratic Tracking Control. J Bioengineer & Biomedical Sci 6: 192. doi:10.4172/2155-9538.1000192

Citation: Korentis GA, Enderle JD (2016) Transitioning from Saccade to Smooth Pursuit Eye Movements using Linear Quadratic Tracking Control. J Bioengineer & Biomedical Sci 6: 192. doi:10.4172/2155-9538.1000192

Methods

Dynamic formulation

Here, we make use of the second order Westheimer model of the oculomotor plant and define the state equations as

$$\dot{\mathbf{x}}(t) = \mathbf{Fx}(t) + \mathbf{Gu}(t) \tag{1}$$

$$\frac{d}{dt}\begin{bmatrix} x_1(t) \\ x_2(t) \end{bmatrix} = \begin{bmatrix} 0 & 1 \\ -\omega_n^2 & -2\zeta\omega_n \end{bmatrix}\begin{bmatrix} x_1(t) \\ x_2(t) \end{bmatrix} + \begin{bmatrix} 0 \\ \dfrac{\omega_n^2}{k} \end{bmatrix} u(t) \tag{2}$$

For a 20° target saccade, Westheimer reported the natural frequency and the damping ratio of the system to be $\omega_n^2 = 120 rad/s$ and $\zeta = 1/\sqrt{2}$ for an eye with a weight of 25 g and a radius of 11 mm [4,7].

Converting to SI units of kg-N-m and solving for the stiffness (k = 0.998), the stability matrix, **F**, and the control-effect matrix, **G**, can be represented numerically such that

$$\frac{d}{dt}\begin{bmatrix} x_1(t) \\ x_2(t) \end{bmatrix} = \begin{bmatrix} 0 & 1 \\ -14,400 & -169.7 \end{bmatrix}\begin{bmatrix} x_1(t) \\ x_2(t) \end{bmatrix} + \begin{bmatrix} 0 \\ 14,424.2 \end{bmatrix} u(t) \tag{3}$$

For this study, instead of limiting the control strategy to only track smooth pursuit eye movements using the LQTC, we added the capability of rapidly positioning the eye to a predicted target location on the trajectory as a priori. This will be accomplished using the open-loop step response of the Westheimer model as shown for various magnitudes in Figure 4.

Timing saccade to smooth transitions

The specific timing characteristics of the saccade are taken directly from the Main Sequence Diagrams. A straight line approximation for the spread of data shown in Figure 3C reveals that saccade latency is relatively constant across all magnitudes and is approximately 175 ms. This will be the value used in our simulations. Saccade duration is linearly proportional to it its magnitude as shown in Figure 3B. From the data, the straight line approximation is calculated to be

$$t_d = .02468 + 0.001739\left|\theta_{target} - \theta_o\right| \tag{4}$$

The saccade duration is an important factor for predicting the time in which the target trajectory will be acquired and helps us decide the time course for switching control strategies.

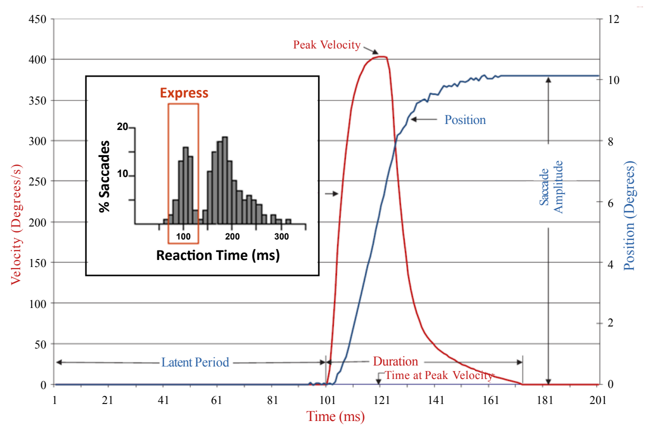

Figure 2: Typical characteristics of an express saccade (Modified from) [4].

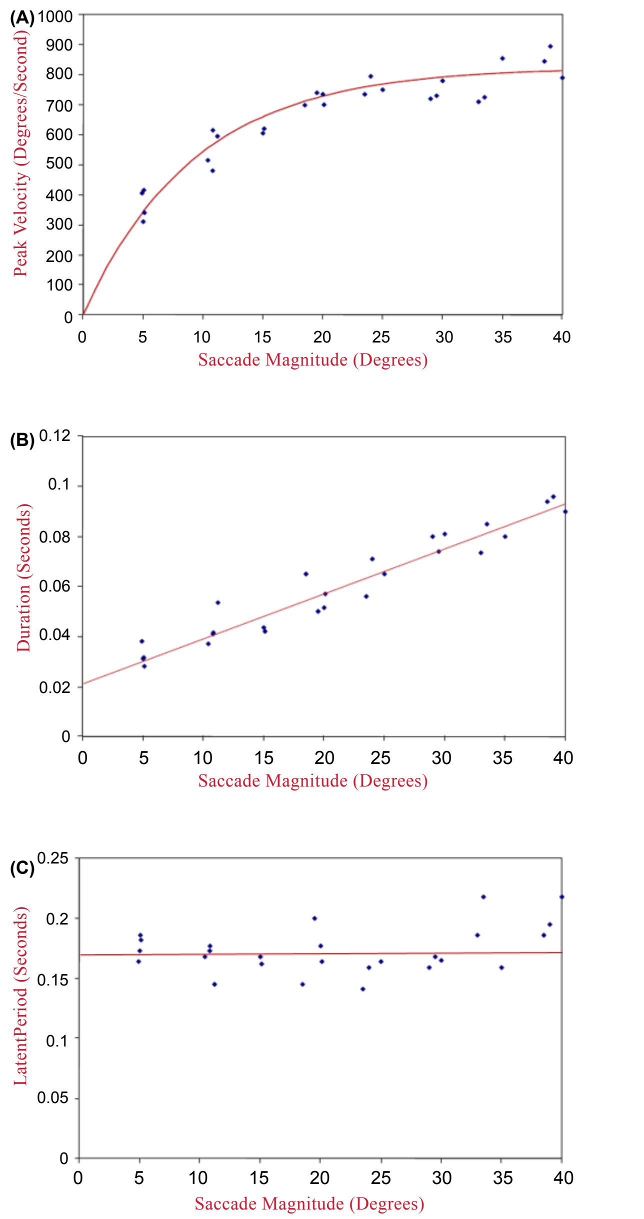

Figure 3: Main Sequence Diagrams for Horizontal Saccades. A) Peak velocity vs. Saccade Magnitude, B) Saccade Duration vs Saccade Magnitude, and C) Latent Period vs Saccade Magnitude. (Adopted from [4]).

Linear quadratic tracking control (LQTC)

Once the eye has been rapidly positioned to the estimated target location of the motion profile, the control strategy must switch from targeting to tracking. In this sense, the optimal control formulation is piecewise continuous. The goal of the tracking portion of the movement is to maintain the system state $\boldsymbol{x}(t)$ as close as possible to the desired state (or reference trajectory) $\boldsymbol{x}_d(t)$ while using minimal control effort in the time interval, $t \in \{t_0, t_f\}$ [20,21]. The optimal control problem for the smooth pursuit portion of the movement is therefore posed the following way:

Find the optimal control $\boldsymbol{u}^*(t)$, for the state-space system given in (2) that tracks a desired trajectory, $\boldsymbol{x}_d(t)$ and minimizes the performance criteria

Citation: Korentis GA, Enderle JD (2016) Transitioning from Saccade to Smooth Pursuit Eye Movements using Linear Quadratic Tracking Control. J Bioengineer & Biomedical Sci 6: 192. doi:10.4172/2155-9538.1000192

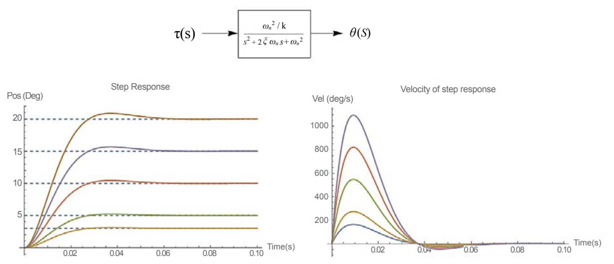

Figure 4: Westheimer step response for various magnitudes.

$$J\left[\boldsymbol{x}(t),\boldsymbol{u}(t),t\right]=\phi\left[\boldsymbol{x}(t_f),t_f\right]+\int_{t_0}^{t_f}\mathcal{L}\left[\boldsymbol{x}(\tau),\boldsymbol{u}(\tau)\right]d\tau$$
$$=\frac{1}{2}[\boldsymbol{x}(t_f)-\boldsymbol{x}_d(t_f)]^T\boldsymbol{P}(t_f)[\boldsymbol{x}(t_f)-\boldsymbol{x}_d(t_f)]+\frac{1}{2}\int_{t_0}^{t_f}\left\{[\boldsymbol{x}(t)-\boldsymbol{x}_d(t)]^T\boldsymbol{Q}[\boldsymbol{x}(t)-\boldsymbol{x}_d(t)]+\boldsymbol{u}(t)^T\boldsymbol{R}\,\boldsymbol{u}(t)\right\}dt \quad (5)$$

subject to the dynamic equality constraint

$$\boldsymbol{f}\left[\boldsymbol{x}(t),\boldsymbol{u}(t),t\right]-\dot{\boldsymbol{x}}(t)=0 \quad (6)$$

where the final time t_f is fixed, the final state, $\boldsymbol{x}(t_f)$, is free to vary and the state and control are not bounded. The terminal state weighting matrix, ***P***, and the state weighting matrix ***Q*** are real, symmetric, positive semi-definite matrices and the control weighting matrix, ***R***, is a real, symmetric, positive definite matrix.

The Hamiltonian for the tracking problem is defined as

$$\mathcal{H}[\boldsymbol{x}(t),\boldsymbol{u}(t),\boldsymbol{\lambda}(t),t]=\mathcal{L}[\boldsymbol{x}(t),\boldsymbol{u}(t),t]+\boldsymbol{\lambda}(t)^T\boldsymbol{f}[\boldsymbol{x}(t),\boldsymbol{u}(t),t] \quad (7)$$

where the Lagrangian is

$$\mathcal{L}\left[\boldsymbol{x}(t),\boldsymbol{u}(t),t\right]=\left[\boldsymbol{x}(t)-\boldsymbol{x}_d(t)\right]^T\boldsymbol{Q}[\boldsymbol{x}(t)-\boldsymbol{x}_d(t)]+\boldsymbol{u}(t)^T\boldsymbol{R}\,\boldsymbol{u}(t) \quad (8)$$

and the augmented state is

$$\boldsymbol{\lambda}(t)^T\boldsymbol{f}\left[\boldsymbol{x}(t),\boldsymbol{u}(t),t\right]=\boldsymbol{\lambda}(t)^T\dot{x}(t)=\boldsymbol{\lambda}(t)^T[\boldsymbol{F}\boldsymbol{x}(t)+\boldsymbol{G}\boldsymbol{u}(t)] \quad (9)$$

The necessary conditions for optimality are

i. State Equations

$$\frac{\partial\mathcal{H}}{\partial\boldsymbol{\lambda}}=\dot{\boldsymbol{x}}(t)=\boldsymbol{F}\boldsymbol{x}(t)+\boldsymbol{G}\boldsymbol{u}(t) \quad (10)$$

ii. Co-State Equations

$$\frac{\partial H}{\partial x}=-\dot{\lambda}(t)=\mathbf{Q}(t)\boldsymbol{x}(t)+\mathbf{F}(t)^T\boldsymbol{\lambda}(t)-\boldsymbol{Q}(t)\boldsymbol{x}_d(t) \quad (11)$$

iii. Optimality Condition

$$\frac{\partial\mathcal{H}}{\partial\boldsymbol{u}}=\boldsymbol{R}\boldsymbol{u}(t)+\boldsymbol{\lambda}(t)^T\boldsymbol{G}(t)=0 \quad (12)$$

The optimal control law as a function of the co-state variable is therefore,

$$\boldsymbol{u}(t)=-\boldsymbol{P}^{-1}\boldsymbol{G}(t)^T\boldsymbol{\lambda}(t) \quad (13)$$

Substituting the optimal control law (13) into the state equations (10) and combining with the co-state equations (11), yields the Hamiltonian system

$$\begin{bmatrix}\dot{x}(t)\\ \dot{e}(t)\end{bmatrix}=\begin{bmatrix}\boldsymbol{F}(t) & -\boldsymbol{G}(t)\boldsymbol{R}^{-1}(t)\boldsymbol{G}^T(t)\\ -\boldsymbol{Q}(t) & -\boldsymbol{F}^T(t)\end{bmatrix}\begin{bmatrix}\boldsymbol{x}(t)\\ \boldsymbol{\lambda}(t)\end{bmatrix}+\begin{bmatrix}0\\ Q(t)\boldsymbol{x}_d(t)\end{bmatrix} \quad (14)$$

Note that this a two-point boundary value problem in which we will need to integrate the co-state variables backwards in time. The terminal boundary conditions are

$$\left\{\frac{\partial\phi[x(t),t]}{\partial t}+\mathcal{H}[\boldsymbol{x}(t),\boldsymbol{u}(t),\boldsymbol{\lambda}(t)]\right\}\Bigg|_{t=t_f}\delta t_f+\left\{\frac{\partial}{\partial x}\phi[\boldsymbol{x}(t_f),t]-\boldsymbol{\lambda}^T(t)\right\}\Bigg|_{t=t_f}\delta x(\delta u)=0 \quad (15)$$

Because the final time is fixed and $\boldsymbol{x}(t_f)$ is free to vary, the following terminal constraint must then be satisfied

$$\boldsymbol{\lambda}^T(t_f)=\frac{\partial}{\partial x}\phi[\boldsymbol{x}(t_f)] \quad (16)$$

The partial derivative of the terminal cost with respect to the state is therefore

$$\boldsymbol{\lambda}(t_f)=\boldsymbol{P}(t_f)[\boldsymbol{x}(t_f)-\boldsymbol{x}_d(t_f)] \quad (17)$$

Assuming (17) holds for the entire interval, such that

$$\boldsymbol{\lambda}(t)=\boldsymbol{P}(t)\boldsymbol{x}(t)-\boldsymbol{P}(t)\boldsymbol{x}_d(t) \quad (18)$$

taking the time derivative

$$\dot{\boldsymbol{\lambda}}(t)=\dot{\boldsymbol{P}}(t)\boldsymbol{x}(t)+\boldsymbol{P}(t)\dot{\boldsymbol{x}}(t)-\dot{\boldsymbol{P}}(t)\boldsymbol{x}_d(t)-\boldsymbol{P}(t)\dot{\boldsymbol{x}}_d(t) \quad (19)$$

and substituting back into (14) yields matrix differential equations of the Riccati form

$$\left[\dot{\boldsymbol{P}}(t)+\boldsymbol{F}^T\boldsymbol{P}(t)+\boldsymbol{P}(t)\boldsymbol{F}-\boldsymbol{P}(t)\boldsymbol{G}\boldsymbol{R}^{-1}\boldsymbol{G}^T\boldsymbol{P}(t)+\boldsymbol{Q}\right]\boldsymbol{x}(t)$$
$$=\boldsymbol{P}(t)\dot{\boldsymbol{x}}_d(t)+[\dot{\boldsymbol{P}}(t)+\boldsymbol{F}^T\boldsymbol{P}(t)-\boldsymbol{P}(t)\boldsymbol{G}\boldsymbol{R}^{-1}\boldsymbol{G}^T\boldsymbol{P}(t)+\boldsymbol{Q}]\boldsymbol{x}_d(t) \quad (20)$$

Here we introduce the tracking variable and its derivative as

$$\boldsymbol{S}(t)=-\boldsymbol{P}(t)\boldsymbol{x}_d(t) \quad (21)$$

$$\dot{\boldsymbol{S}}(t)=-\dot{\boldsymbol{P}}(t)\boldsymbol{x}_d(t)-\boldsymbol{P}(t)\dot{\boldsymbol{x}}_d(t) \quad (22)$$

Substituting (21) and (22) into (20) results in

$$\left[\dot{\boldsymbol{P}}(t)+\boldsymbol{F}(t)^T\boldsymbol{P}(t)+\boldsymbol{P}(t)\boldsymbol{F}(t)-\boldsymbol{P}(t)\boldsymbol{G}(t)\boldsymbol{R}^{-1}(t)\boldsymbol{G}^T(t)\boldsymbol{P}\right.$$
$$+\{\dot{\boldsymbol{S}}(t)+[\boldsymbol{F}(t)^T-\boldsymbol{P}(t)\boldsymbol{G}(t)\boldsymbol{R}^{-1}(t)\boldsymbol{G}^T(t)]\boldsymbol{S}(t)-\boldsymbol{Q}(t)\boldsymbol{x}_d(t)\}=0 \quad (23)$$

The optimal state and desired trajectory cannot be zero throughout the entire interval, therefore (23) can be partitioned into two separate equations and integrated independently.

$$\dot{\boldsymbol{P}}(t)+\boldsymbol{F}(t)^T\boldsymbol{P}(t)+\boldsymbol{P}(t)\boldsymbol{F}(t)-\boldsymbol{P}(t)\boldsymbol{G}(t)\boldsymbol{R}^{-1}(t)\boldsymbol{G}^T(t)\boldsymbol{P}(t)+\boldsymbol{Q}(t)=0 \quad (24)$$

$$\dot{\boldsymbol{S}}(t)+[\boldsymbol{F}(t)^T-\boldsymbol{P}(t)\boldsymbol{G}(t)\boldsymbol{R}^{-1}(t)\boldsymbol{G}^T(t)]\boldsymbol{S}(t)-\boldsymbol{Q}(t)\boldsymbol{x}_d(t)=0 \quad (25)$$

Rewriting the terminal condition for the tracking variable from (17) is simply

$$\boldsymbol{S}(t_f)=-\boldsymbol{P}(t_f)\boldsymbol{x}_d(t_f) \quad (26)$$

The optimal control law (13) is now written in terms of the Riccati variables and tracking variables, which can be further simplified into a feedback gain matrix, ***K***(t), and a command signal, $\boldsymbol{v}(t)$,

$$\boldsymbol{u}^*(t)=-\boldsymbol{R}^{-1}\boldsymbol{G}(t)^T\boldsymbol{P}(t)\boldsymbol{x}(t)-\boldsymbol{R}^{-1}\boldsymbol{G}(t)^T\boldsymbol{S}(t)$$
$$\triangleq\boldsymbol{K}(t)\boldsymbol{x}(t)+\boldsymbol{v}(t) \quad (27)$$

Qualification

The main premise for the tracking controller is for producing the optimal control law that would faithfully represent the input to the system given a desired trajectory to track. To qualify the model, we will track the output trajectory of a 20° saccade produced by the Westheimer model in response to a step input of 20 with zero neural transmission delay.

Citation: Korentis GA, Enderle JD (2016) Transitioning from Saccade to Smooth Pursuit Eye Movements using Linear Quadratic Tracking Control. J Bioengineer & Biomedical Sci 6: 192. doi:10.4172/2155-9538.1000192

As shown in Figure 5 the LQTC follows the target trajectory with no error and reproduces the control used to force the Westheimer output response. This was achieved by experimenting with the state-weighting matrix values of $\boldsymbol{Q}$. It should be noted that the model quickly goes unstable with state feedback delay of 150 ms. This result is not surprising however, since saccades operate in an open-loop fashion and are not affected by neural transmission delays.

Saccade to smooth pursuit control

Figure 5 shows the implementation of the saccade branch to the LQTC. Based on an internal representation of the system's boundary conditions and operating parameters (i.e. it has an intimate knowledge of its latency), higher level motor centers estimate the time and magnitude of target acquisition. It compares this value to an estimate of the eye's current position and determines whether to elicit a saccade or to smoothly track the motion profile. If the choice is to *move fast*, feedback is inhibited for the duration of the movement which is computed using (4). The time of interception, or the time in which the eye has successfully moved from targeting to tracking, is defined as

$$t_{Acq} = t_{lat} + t_d \tag{28}$$

Where

t_{lat} is the latent period prior to the saccade and determined to be 175 ms from Figure 3C t_d is the duration of the saccade which is calculated using (4).

Application development

A real-time application was developed using Wolfram Mathematica to simulate the response of a saccade to smooth pursuit transition. The user may select from various waveforms with the ability to choose from different magnitudes, initial eye positions and frequencies. State, control and terminal-state weighting matrices can be inputted directly to evaluate the LQTC performance for the smooth pursuit portion of the movement. The user may increase the position feedback delay gradually to effectively test the stability based on the chosen parameters. Four different plots are available as a visual aid to the designer. The state plot gives the response in terms of eye position and velocity. The phase option shows the phase portrait of the states and the Lyapunov stability of the system. The control selection shows a plot of the optimal control computed for the system. Finally, the MDRE option allows the designer to see both time courses of the numerically integrated Riccati and Tracking variables.

Results

The following plots reflect the smooth transition between a saccade and a smooth pursuit eye movement, for various motion profiles, with a pure position feedback delay of 150 ms. The state weighting, control weighting and terminal state weighting matrices used for the LQTC are as follows.

$$\boldsymbol{Q} = \begin{pmatrix} 15 & 5 \\ 5 & 60 \end{pmatrix}; r = 1; \boldsymbol{P}(t_f) = \begin{pmatrix} 1 & 0 \\ 0 & 0 \end{pmatrix} \tag{29}$$

Overall, these weighting values provided the best all-around tracking performance for the continuous waveforms tested across frequencies up to 1 Hz.

Ramp targeting and tracking

Pursuit Trajectory = 5 + 20*t* ; *Initial Eye Position* = -5°

Here we will take a closer look at the saccade portion of the

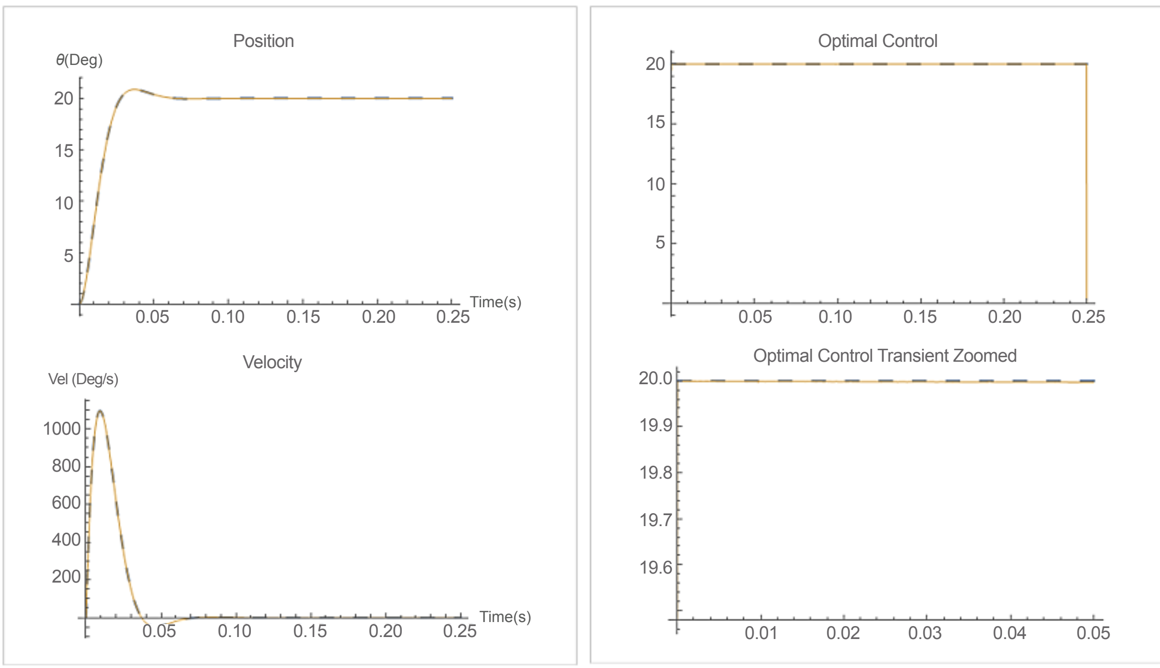

$$Q=\begin{bmatrix} 1.0 & 0 \\ 0 & 100 \end{bmatrix}; r = 1; P(t_f)=\begin{bmatrix} 1 & 0 \\ 0 & 0 \end{bmatrix}$$

Figure 5: LQTC perfect tracking and reproduction of original control input.

Citation: Korentis GA, Enderle JD (2016) Transitioning from Saccade to Smooth Pursuit Eye Movements using Linear Quadratic Tracking Control. J Bioengineer & Biomedical Sci 6: 192. doi:10.4172/2155-9538.1000192

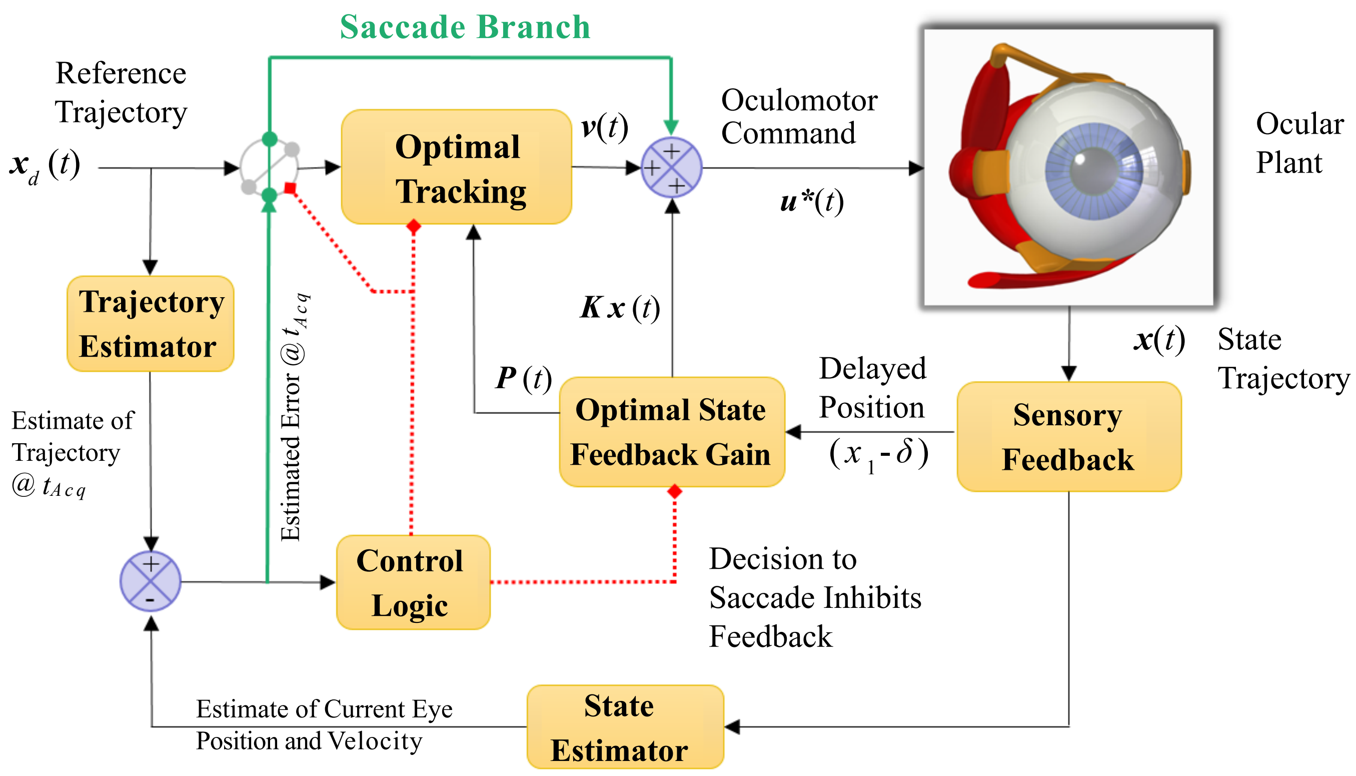

Figure 6: Switching control methodology between saccades and smooth pursuit with LQTC.

movement and see how it correlates to the main sequence diagrams. Referring to Figures 6-8, starting at an initial position of -5° we see that the saccade latency is 175 ms which is consistent with Figure 3C. The saccade magnitude computed for the movement was 14.458° and had duration of 48.16 ms. Evaluating the straight line approximation of Figure 3B, we can see that the duration for a 15° saccade is just under 50 ms. The peak velocity of the simulated saccade was 544.2°/s and differs from the approximate value of 625°/s taken from Figure 3A.

The optimal control computed using the LQTC after the saccade is compared for the case of no delay and a neural transmission delay of 150 ms as shown in Figure 9.

For the interesting case of a trajectory passing through the line of site, the following ramp function was defined.

Pursuit Trajectory = 5 - 20*t*; *Initial Eye Position* = -3°

Cosine targeting and tracking

Pursuit Trajectory = 20 *Cos*(π t); *Initial Eye Position* = 3°

Sum of Sines

$$Pursuit\,Trajetory = -20\,[Sin\left(\frac{\pi}{2}t\right) + Sin(\pi t)];\,Initial\,Eye\,Position = 5°$$

Product of Sines

$$Pursuit\,Trajetory = 15\,[Sin\left(\frac{\pi}{2}t\right)Sin(\pi t)];\,Initial\,Eye\,Position = 3°$$

Discussion

The LQTC is an effective optimal control strategy that compensates for neural transmission delays of 150ms and produces minimal error tracking [1]. Using a unimodal control approach in which the LQTC functions to both target and pursue a reference trajectory, accurate tracking is achieved but not within a reasonable time course when the position of the eye is initially offset from the trajectory as shown in Figure 1.

However, the results clearly show that implementing a saccade to target a motion profile prior to tracking it greatly improves the time in which the LQTC can synchronize its position and velocity profiles to that of the pursuit trajectory (Figures 8,10,11,13,16 and 19). The simulation results of this dual mode control strategy directly correspond to the experimental data [2,3,22].

The addition of the saccade to the existing LQTC construct (Figure 6) was intuitively piecewise continuous since the performance criteria for each movement type is different. Saccades function to reposition the eye to a target in the least time possible in the absence of feedback while smooth pursuits, which are subject to the destabilizing effects of neural transmission feedback delays, strive to minimize the error between the desired and state trajectories while trading control energy expenditure to do it.

Saccade simulations

Fast eye movements work in an open loop mode in which feedback is absent. This is supported by the fact that our visual perception and proprioceptive feedback is temporarily disabled for the duration of the saccade [4,5]. The mode of operation is that of targeting. The following table summarizes the results for the saccade portion of the movement simulation for each pursuit trajectories (Figures 9,12,14,15,17 and 20) and compares the results with the experimental values of the main sequence diagrams (Figure 3).

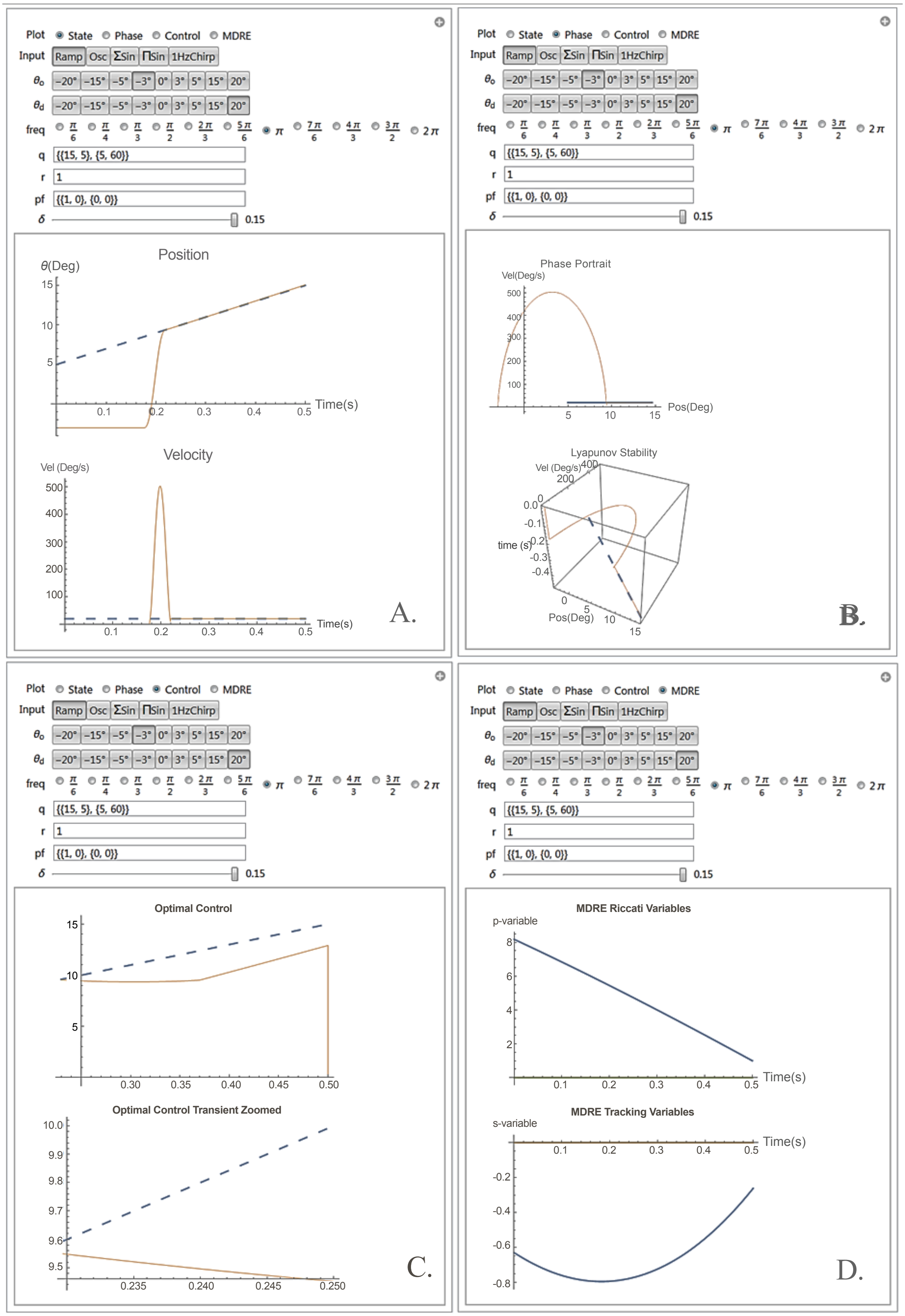

Figure 7: Saccade2Smooth Pursuit LQTC Application, A) State Plots, B) Phase and Lyapunov Plots, C) Tracking Optimal Control, D) MDRE Riccati and Tracking Time Response.

Citation: Korentis GA, Enderle JD (2016) Transitioning from Saccade to Smooth Pursuit Eye Movements using Linear Quadratic Tracking Control. J Bioengineer & Biomedical Sci 6: 192. doi:10.4172/2155-9538.1000192

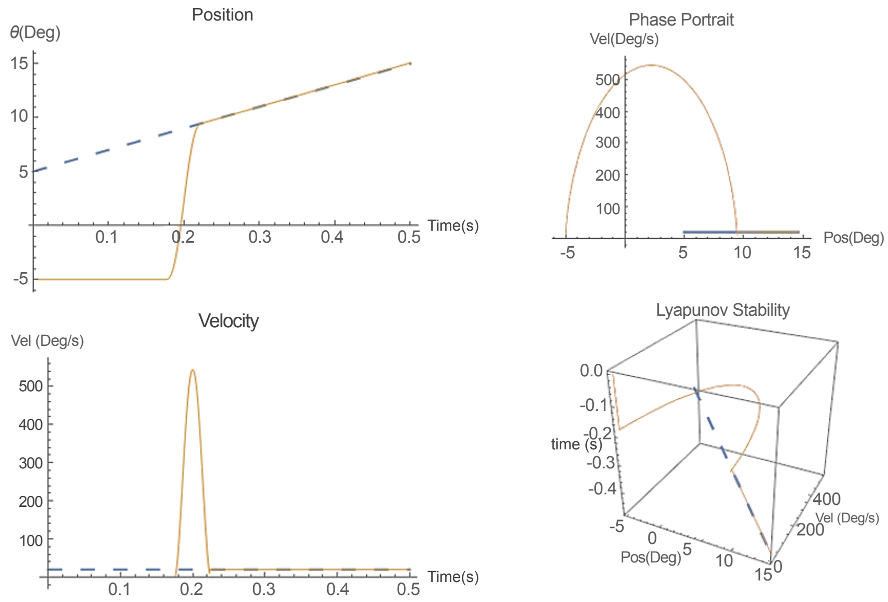

Figure 8: Ramp targeting and tracking starting at a negative initial position.

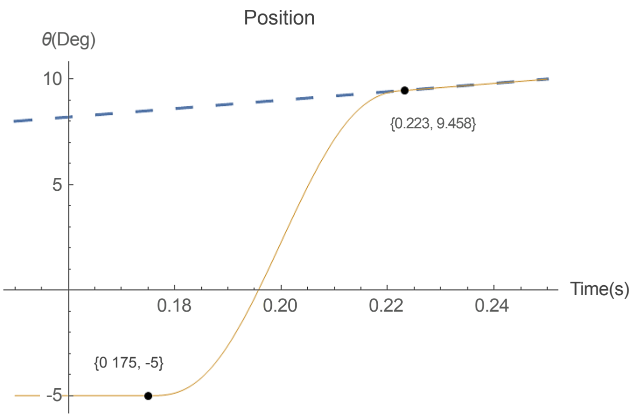

Figure 9: Ramp targeting, saccade zoomed, illustrating the latency, initial eye position, final position and time of target acquirement. The simulated values directly correlate to the Main Sequence Diagrams.

The duration of the simulated saccade movement has excellent correspondence to the main sequence diagrams. However, peek velocity is smaller in all cases with exception to the crossing profile of the negatively pursuing ramp function. As noted previously, based on an internal representation of the system, the latency is known to the controller and hard coded to be 175ms (Figure 3C).

One reason for the difference in values for peek velocity may be attributed to the simple second order model used to describe the dynamics of the plant. A better model that incorporates an antagonist muscle pair with separately maintained neural innervation, such as those reported by Enderle, et al. [12,23], may help with further investigation regarding the smooth transition between the targeting of a saccade and tracking of a smooth pursuit eye movement. Since muscle acts as a neuromuscular-actuator with non-zero output mechanical impedance and because antagonist muscle pairs are co-activated, incorporating the model may provide effects similar to feedback action without being vulnerable to the destabilizing effects of neural transmission delays [20-22].

Smooth pursuit simulations

The implementation of the LQTC clearly shows the ability to effectively handle realistic neural transmission delays of 150 ms and track various motion profiles with zero latency. The results are directly supported with experimental observations [24].

Optimal control: Referring back to the optimal control law (27), the command signal, $\boldsymbol{v}(t)$, depends on system parameters and future

Citation: Korentis GA, Enderle JD (2016) Transitioning from Saccade to Smooth Pursuit Eye Movements using Linear Quadratic Tracking Control. J Bioengineer & Biomedical Sci 6: 192. doi:10.4172/2155-9538.1000192

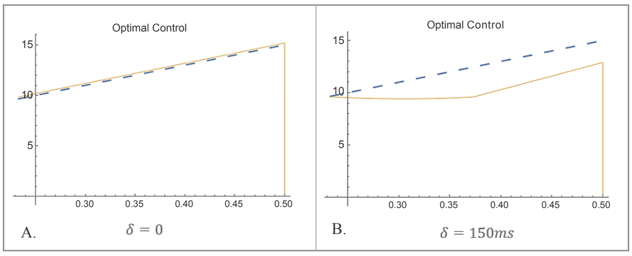

Figure 10: LQTC Optimal Control A) No Delay, B) 150ms Delay.

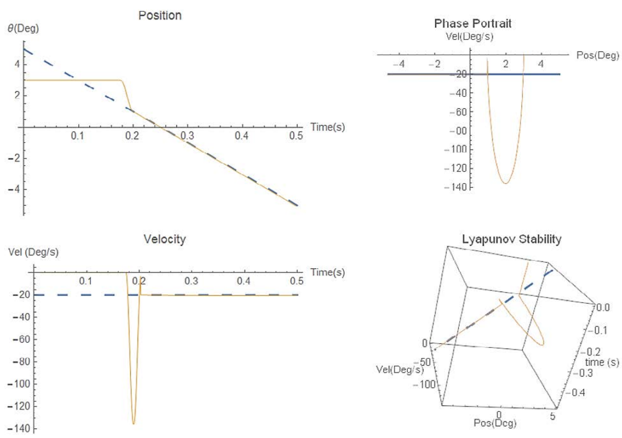

Figure 11: Ramp targeting and tracking, special case of the trajectory crossing the line of site.

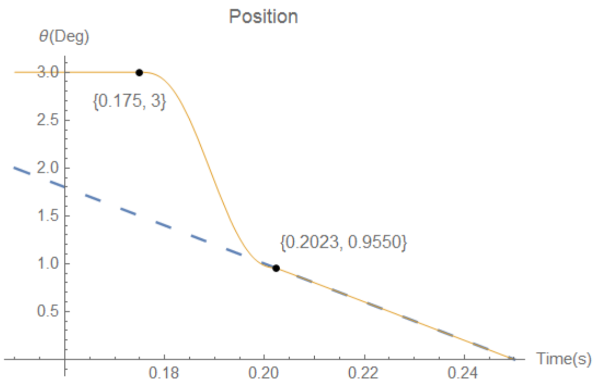

Figure 12: Ramp targeting, crossing the line of site, saccade to smooth transition, zoomed.

values of the reference trajectory, $\boldsymbol{x}_d(t)$. Having this knowledge as a priori, we can anticipate where we intend to go based on the current state of the system. This statement is directly supported by observing the optimal controls computed for the A) zero delay case, and the B) 150 ms delay case of Figures 10,15,18 and 21. For both cases, the LQTC effectively tracks the pursuit trajectory. The major difference is the optimal control required to do it. The optimal control computed for the zero delay case is an exact replica of the desired trajectory. In contrast, the optimal control for the delayed case leads the input to account for the neural transmission delay because it has prior knowledge of not only the trajectory to be tracked but also the current state of the system. In essence, the LQTC uses an internal representation of the system state and makes adjustments to improve behavioral performance [25-27].

Weighting effects

The effectiveness of the LQTC is driven by the performance criteria specified in (5) which establishes tradeoffs between state and control. The state-weighting matrix, $\boldsymbol{Q}$, specifies the relative importance between each state while the control-weighting matrix, $\boldsymbol{R}$, establishes the permissible energy expenditure (a scalar value in this study). Here

Citation: Korentis GA, Enderle JD (2016) Transitioning from Saccade to Smooth Pursuit Eye Movements using Linear Quadratic Tracking Control. J Bioengineer & Biomedical Sci 6: 192. doi:10.4172/2155-9538.1000192

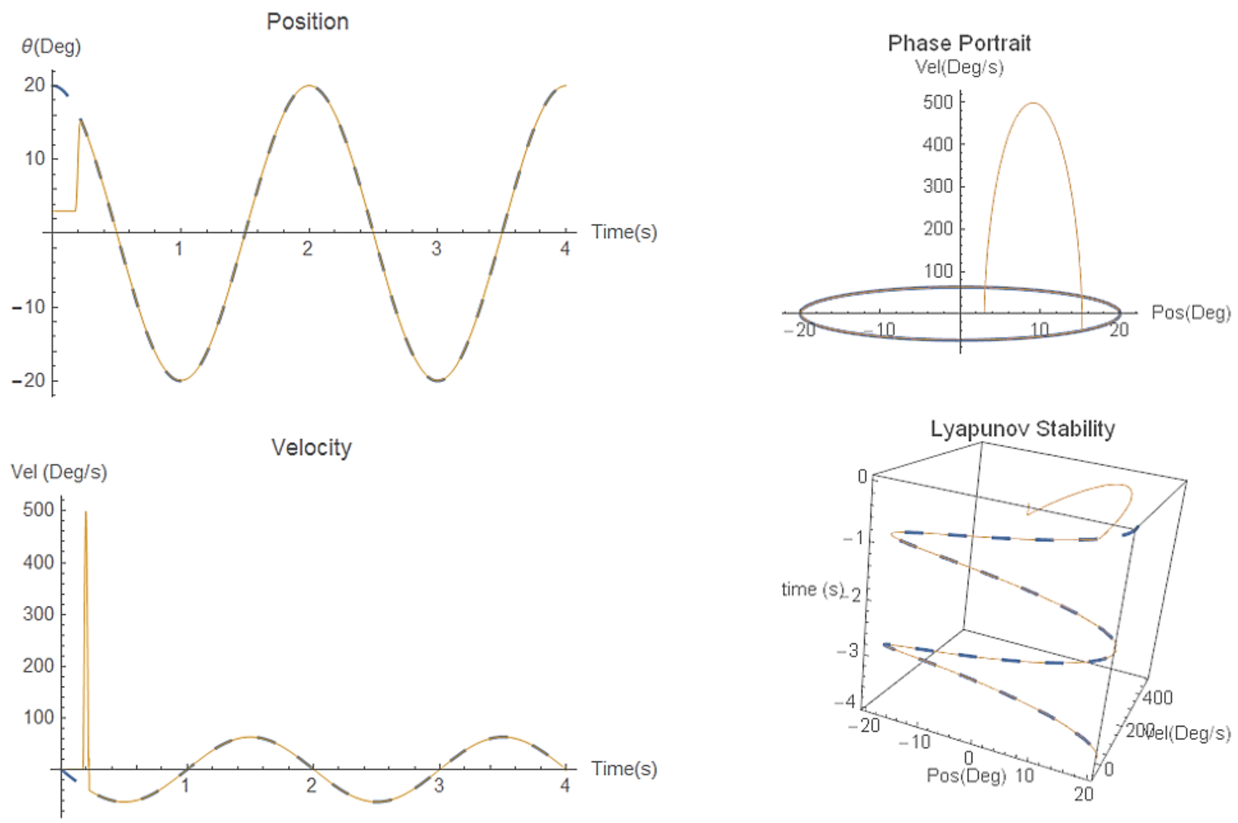

Figure 13: Cosine targeting and tracking.

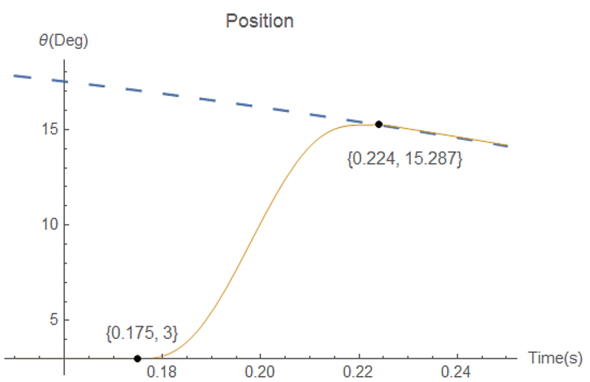

Figure 14: Cosine targeting, saccade to smooth transition, zoomed.

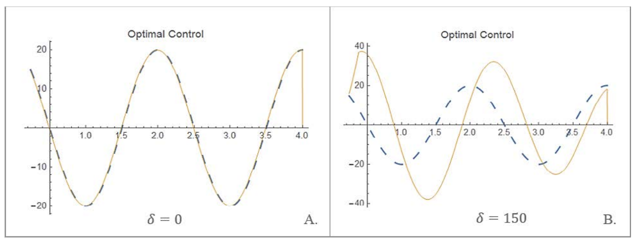

Figure15: Optimal Control for Cosine A) No Delay, B) Delay of 150ms.

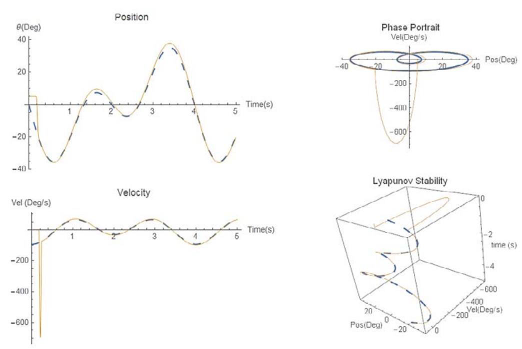

Figure 16: Sum of Sines targeting and tracking.

we will evaluate the effects of the weights on the targeting and tracking portions of the movement. Since the goal is to accurately track a desired trajectory while accommodating a 150 *ms* feedback delay, we will first evaluate the effects of weighting on the smooth pursuit portion of the movement.

Smooth pursuit: Consider the response of the LQTC with different state-weighting factors for an oscillatory input at different frequencies as shown in Figure 22. The relative tradeoff between position and velocity performance for different frequencies is a direct result of the weight-

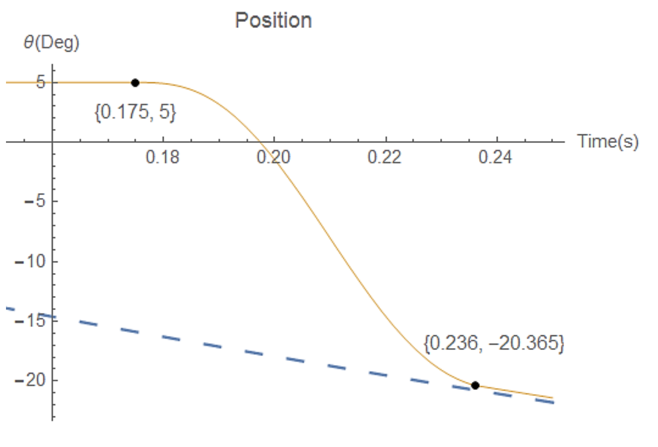

Figure 17: Sum of Sines targeting, saccade to smooth transition, zoomed.

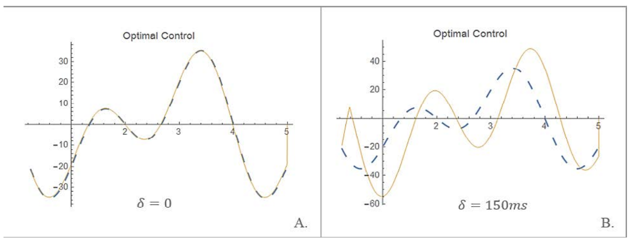

Figure 18: Optimal Control for Sum of Sines A) No Delay, B) Delay of 150ms.

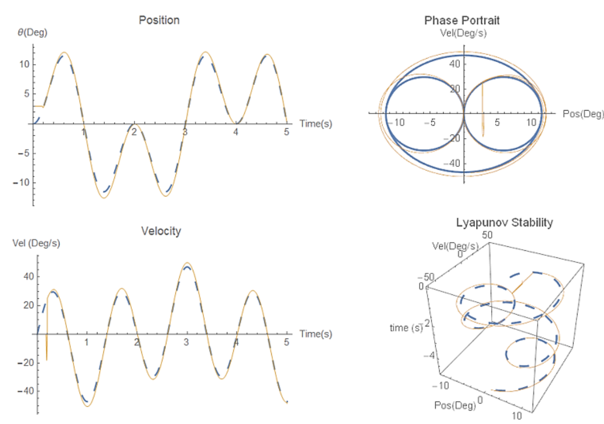

Figure 19: Product of Sines targeting and tracking.

ing values and readily apparent by inspection.

Careful experimentation with different weighting values for multiple waveforms at different frequencies resulted in the values presented in (29). The effect of penalizing velocity more heavily than position, along with weighting the coupling between them, resulted in exceptional tracking performance for the smooth pursuit portion of the movement.

Saccade

As shown in Figure 5, the LQTC can be used to track a saccade produced by the step response of the Westheimer model. Additionally,

Pursuit Trajectory	Movement Mag (Deg)	SIM	MSD	SIM	MSD
		Duration (sec)		Peek Velocity	
5 + 20*t*	14.458	.048	.048	544	625
5 - 20*t*	-2.045	.027	.027	138	125
20 Cos(*t*)	12.287	.049	.046	498	600
$-20\ [Sin\left(\frac{\pi}{2}t\right)+Sin(\pi t)];$	-25.365	.061	.062	694	750
$15\ [Sin\left(\frac{\pi}{2}t\right)Sin(\pi t)];$	-0.246	.026	.028	19	25

Table 1: Comparison of simulated saccades with main sequence diagrams.

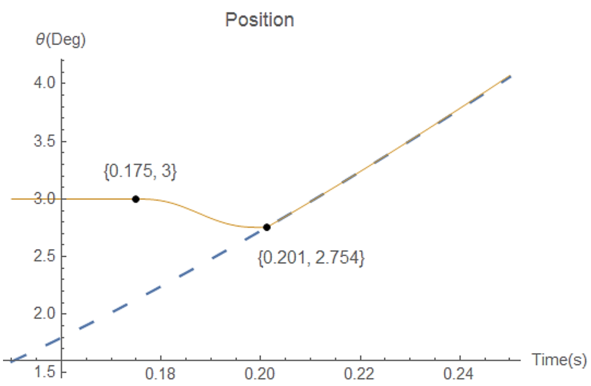

Figure 20: Product of Sines targeting, saccade to smooth transition, zoomed.

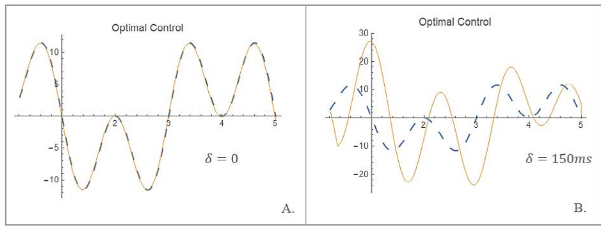

Figure 21: Optimal Control for Product of Sines A) No Delay, B) Delay of 150ms.

it computes an optimal control that reproduces the original step input to the system. However, in order to achieve this objective, the values selected for the weights had to be different from those presented in (29) which were used for the smooth pursuit portion of the movement. For example, Figure 23 shows the tracking performance for three pursuit motion profiles using the two sets of weights. This suggests that the oculomotor system may modulate the weighting factors of the control to accommodate the specific motion objective, that is, to either move fast or to track accurately.

To further explore this notion, we test the tracking performance of a step input with different weight sets and by gradually increasing the delay. In order to produce a 20° saccade that has a peak velocity consistent with the main sequence diagrams, the penalty on the position of the movement has to be much higher than on velocity as shown in Figure 24A. Similarly, if we use the LQTC to simulate a saccade with the

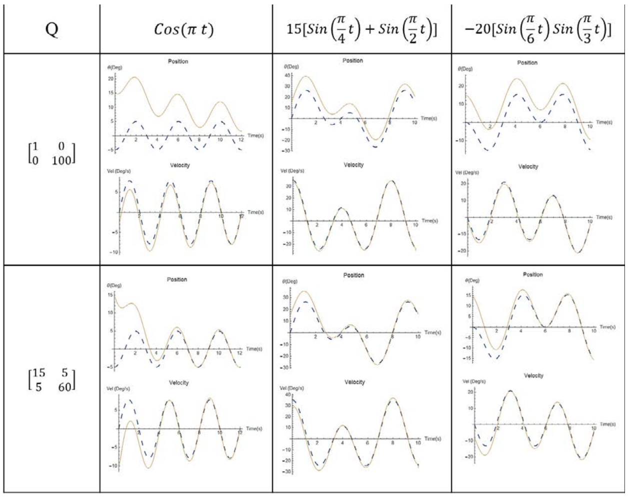

Figure 23: Comparison of the weights used for the saccade and the smooth pursuit of various trajectories.

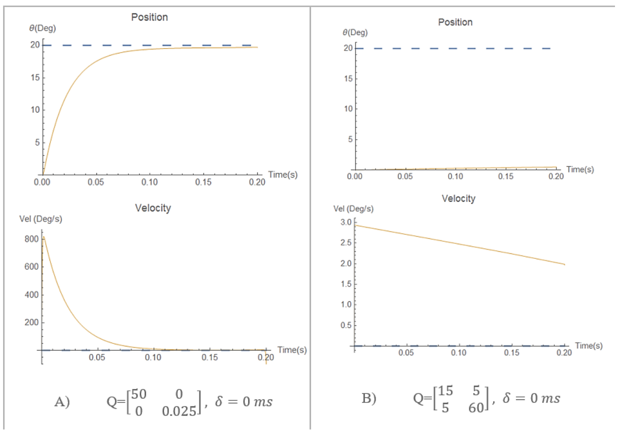

Figure 24: LQTC step response for, A) heavier weight on position, B) weight set used for tracking.

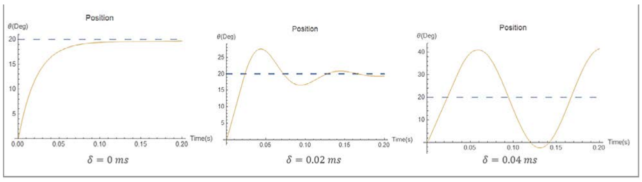

Figure 25: Effects of increasing neural transmission delay.

weighting values presented in (29) the response is negligible.

Finally, as delay is introduced into the position feedback for the weighting values shown in Figure 24A, the stability of the system starts to deteriorate, becoming more oscillatory and quickly growing without bound (Figure 25). These results further support the dual mode control strategy which is specific to either targeting or tracking a desired trajectory.

Conclusion

The addition of a saccade, to rapidly reposition the eye to an estimated target location on the motion profile, greatly enhances the time course in which the LQTC can track the desired trajectory with minimal error and in the presence of large neural transmission delays. The performance criteria for the movement clearly must change from that of a targeting system, which penalizes the time to acquire the target, to that of a tracking system which penalizes a tradeoff between control energy usage and perturbations from the difference between the actual state and desired state trajectories.

Acknowledgment

This work is financially supported in part by QCI, Inc. of Seekonk, MA

References

1. Korentis GA, Enderle JD (2016) Linear Quadratic Tracking Control of Smooth Pursuit Eye Movements. J Biomed Eng Med Devic 1: 112.
2. Spering M, Schütz AC, Braun DI, Gegenfurtner KR (2011) Keep your eyes on the ball: Smooth pursuit eye movements enhance prediction of visual motion. J Neurophysiol 105: 1756-1767.
3. Bahill AT, McDonald JD (1983) Smooth pursuit eye movements in response to predictable target motions. Vision Res 23: 1573-1583.
4. Enderle JD (2010) Models of horizontal eye movements: part 1. Early Models of Saccades and Smooth Pursuit. Morgan & Claypool 163.
5. Purves D (2008) Neuroscience. 4th ed. Sunderland, Mass: Sinauer.
6. Krauzlis RJ (2005) The control of voluntary eye movements: New perspectives. Neuroscientist 11: 124-137.
7. Enderle JD, Blanchard SM, Bronzino JD (2000) Introduction to biomedical engineering. San Diego: Academic Press 1062.
8. Enderle JD, Wolfe JW, Yates JT (1984) The linear homeomorphic saccadic eye movement model--a modification. IEEE Trans Biomed Eng 31: 717-720.
9. Enderle JD, Engelken EJ, Stiles RN (1990) Additional developments in oculomotor plant modeling. Biomed Sci Instrum 26: 59-65.
10. Enderle JD, Wolfe JW (1987) Time-optimal control of saccadic eye movements. Biomedical Engineering, IEEE Transactions on 43-55.
11. Enderle JD (2002) Neural control of saccades. Prog Brain Res 140: 21-49.
12. Enderle JD, Zhou W (2010) Models of horizontal eye movements, part II A 3rd order linear saccade model. Morgan & Claypool Publishers 159.
13. Ghahari A, Enderle JD (2014) Models of horizontal eye movements: part 3, A Neuron and Muscle Based Linear Saccade Model. Morgan & Claypool Publishers 158.
14. Zhai X, Che C, Mazzarese BD, Colberg AV, Enderle JD (2016) A neural control model for horizontal visual, auditory Visual Bisensory Stimuli Elicited Saccades. J Bioeng Biomed Sci S3: 2-12.
15. Clark M, Stark L (1975) Time optimal behavior of human saccadic eye movement. Automatic Control, IEEE Transactions on 20: 345-348.
16. Bergeron A, Matsuo S, Guitton D (2003) Superior colliculus encodes distance to target, not saccade amplitude, in multi-step gaze shifts. Nat Neurosci 6: 404-413.
17. Sparks DL (2002) The brainstem control of saccadic eye movements. Nature Reviews Neuroscience 3: 952-964.
18. Moschovakis AK, Scudder CA, Highstein SM (1996) The microscopic anatomy and physiology of the mammalian saccadic system. Prog Neurobiol 50: 133-254.
19. Bahill A, Clark M, Stark L (1975) The main sequence, a tool for studying human eye movements. Math Biosci 24: I-204.
20. Kirk DE (1970) Optimal control theory: an introduction. Englewood Cliffs, NJ: Prentice-Hall.
21. Stengel RF (1994) Optimal control and estimation.
22. Orban de Xivry JJ, Lefèvre P (2007) Saccades and pursuit: Two outcomes of a single sensorimotor process. J Physiol 584: 11-23.

23. Ghahari A, Enderle JD (2014) A neuron-based time-optimal controller of horizontal saccadic eye movements. Int J Neural Syst 24: 1450017.

24. Hogan N (1984) Adaptive control of mechanical impedance by coactivation of antagonist muscles. IEEE Transactions on Automatic Control 29: 681-690.

25. Farahat W, Herr H (2005) An apparatus for characterization and control of isolated muscle. Neural Systems and Rehabilitation Engineering, IEEE Transactions 13: 473-481.

26. Hollerbach JM, Hunter IW, Ballantyne J (1992) A comparative analysis of actuator technologies for robotics. The robotics review 2 table of contents 299-342.

27. McHugh DE, Bahill AT (1985) Learning to track predictable target waveforms without a time delay. Invest Ophthalmol Vis Sci 26: 932-937.